Werk

Jahr: 1979
Kollektion: fid.geo
Signatur: 8 Z NAT 2148:46
Digitalisiert: Niedersächsische Staats- und Universitätsbibliothek Göttingen
Werk Id: PPN1015067948_0046
PURL: http://resolver.sub.uni-goettingen.de/purl?PPN1015067948_0046

LOG Id: LOG_0012
LOG Titel: Empirical model of global electron temperature distribution between 300 and 700 km based on data from aeros-a
LOG Typ: article

Übergeordnetes Werk

Werk Id: PPN1015067948
PURL: http://resolver.sub.uni-goettingen.de/purl?PPN1015067948
OPAC: http://opac.sub.uni-goettingen.de/DB=1/PPN?PPN=1015067948

Empirical Model of Global Electron Temperature Distribution Between 300 and 700 km Based on Data From Aeros-A[*]

K. Spenner and R. Plugge

Institut für physikalische Weltraumforschung der FhG, D-7800 Freiburg, Federal Republic of Germany

Abstract. An empirical model function of the global electron temperature distribution has been determined based on the measurements of the planar Retarding Potential Analyzer on-board the Aeros-A satellite. The model represents the mean temperature between 300 and 700 km altitude at 0300 LT and 1500 LT depending on latitude, longitude, and height. The model values are compared with all the measured data to show the accuracy achieved and the mean spread of the data for different latitudes. A clear correlation was not found between the electron temperature and geophysical indices such as K_p or sunspot number for the period of low solar activity between January and August, 1973. Seasonal and annual effects could not be detected. The mathematical background and method used to generate the model function is described in the appendix.

Key words: Ionosphere − Electron temperature − Satellite observations − Retarding potential analyzer.

Introduction

The electron temperature shows a characteristic global pattern. The distribution is sometimes masked by geophysical events. However, averaged data show clearly a quite constant pattern as measured by different satellites (Brace, 1970; Dorling and Raitt, 1976; Spenner et al., 1978). In the last ten years a large quantity of temperature data has become available and only a small part of them could be published. A review of the available observations in the *F*-region was recently given by Schunk and Nagy (1978).

An effective way to handle large amounts of data and to extract an average distribution from them can be achieved by modeling measurements by analytical functions. A representative model allows one to compare different sets of data in a quite general form and is useful in predicting mean values. A global

---

[*] Dedicated to Professor Dr. K. Rawer on the occasion of his 65th birthday

temperature model has been generated with ESRO-4 data (Dorling and Raitt, 1976). It shows the dependence of the temperature distribution on altitude, latitude and local time, but it does not show a longitudinal dependence.

We will present in this paper an additional analytical model of the electron temperature. For this purpose we use the data of the planar Retarding Potential Analyzer (Spenner et al., 1974) on-board the AEROS satellite. The satellite was in orbit between December, 1972 and August, 1973 with an apogee of 800 km and a perigee of 240 km. Its path was approximately polar (97°) covering nearly the whole globe. The sun synchronous orbit allowed us to always achieve temperature data at 0300 LT and 1500 LT. Therefore, the AEROS orbit is ideal for investigating a longitudinal structure at constant local time. The model provides the mean electron temperature distribution in concise form representing more than 10,000 measurements.

Model Functions

The model must describe the temperature as a function of the latitude θ, longitude ϕ and height h. The model function $T(h, \theta, \phi)$ can be expressed by spherical harmonics in the form

$$T(h, \theta, \phi) = \sum_{k=0}^{K} \sum_{n=0}^{N} \sum_{m=-n}^{n} a_{knm} \cdot Y_{nm}(\theta, \phi) \cdot F_k(h) \tag{1}$$

where a_{knm} are parameters of series expansion in spherical harmonics, $Y_{nm}(\theta, \phi)$ spherical harmonics, $F_k(h)$ height functions.

Such a sum describes any complex distribution in a worldwide form. The number of necessary terms K, and N depends on the particular distribution and on the desired accuracy.

The parameters a_{knm} can be determined from the relation

$$a_{knm} = \int_h \int_\phi \int_\theta T_M \, Y_{nm} \, F_k \, d\tau \tag{2}$$

where T_M is the measured temperature and $d\tau$ is a space element of the considered volume. A detailed deduction of Eqs. (1) and (2) is shown in the Appendix.

To some extent a similar attempt to model atmospheric parameters was chosen by the OGO-6 model, which describes neutral temperature and composition (Hedin et al., 1974). It also uses spherical harmonics to describe the latitudinal distributions. However, the longitudinal distribution was not considered, and the height function was not determined in the form described here.

The time dependence is not introduced in Eq. (1) because all available data belong to two constant local times. We determine separately two sets of parameters for day- and nighttime according to Eq. (2). Other possible variations such as seasonal, geomagnetic or solar activity variations are not introduced at this stage. These variations will be analyzed separately in a later section. Therefore, all measurements were used in the analysis without any preselection for special geophysical conditions.

Data Basis

The AEROS Retarding Potential Analyzer was designed to measure a temperature in half a second with a repetition period of 18 s determined by telemetry capacity. This measuring interval provided at least one value within every degree of latitude. Because of problems with the satellite-born triggering system only a few orbits are available with a resolution of one degree. Most of the measurements have a resolution of 10 degrees. The data are measured during complete orbit revolutions. Every second or third orbit was recorded. The data coverage was almost homogeneously distributed in longitude and latitude during a period of some days. However, it took three months to achieve data at all heights between apogee and perigee.

All data measured during the first 100 days of 1973 were grouped in ranges of 10° latitude, 60° longitude and 100 km altitude. The relatively wide longitudinal range was chosen to get at least 10 measurements in each cell. The center of the longitudinal cells was shifted in steps of 10°, to get 36 longitudinal cells. One measurement was always contributed to 6 different longitudinal cells centered at 10° longitude and latitude and at 100 km levels between 300 and 700 km. The particular temperature data in each of the 3070 cells were averaged. Standard deviations were calculated separately for each cell. Data being outside of two standard deviations were not used in order to suppress possible runaways under unfavorable conditions. The relatively small amount of data in each cell and the sometimes quite large temporal changes of the electron temperature suggested that the mean temperature in each range be smoothed by a running weighted average between cells directly adjacent in latitude and height. These smoothed data are assigned $T_M(\theta, \phi, h)$.

Calculation of the Model

In the beginning we used three coordinate systems: geographic, geomagnetic and modified dip coordinates. For each system the standard deviations in all the particular cells were determined and averaged. The smallest mean standard deviation was by far achieved in the geomagnetic system. This suggests that the geomagnetic system gives the most appropriate description. Therefore, further analysis is done only with geomagnetic coordinates.

The parameter a_{knm} were calculated with Eq. (2). The integral was replaced by a sum over the 3070 cells. The appropriate order of the series expansion was determined by a comparison between the model function $T(N, K)$ with the mean temperatures T_M in the particular cells. The mean deviation d, which is given by

$$d = \frac{\Sigma \delta \pm \Sigma |\delta|}{n} \tag{3}$$

where $\delta = (T_M - T) \, T^{-1}$ and n is number of measurements, is shown in Fig. 1 as a function of N, the highest order of spherical harmonics, for $K = 3$. A third order approximation in height h is necessary to reproduce the temperature maximum
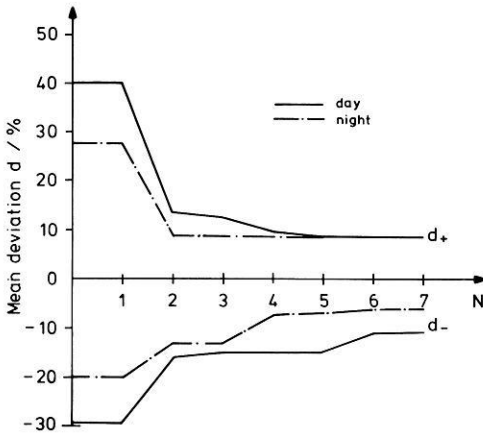
Fig. 1. Deviation between observed mean temperatures and the order N of the model function

at low altitudes in the equatorial area. However, analyzing the height-profile of temperature at a fixed location – except low latitudes – it is usually sufficient to describe T as a linear function of height h. Fig. 1 indicates that the highest useful order for N is 6.

A higher number of parameters did not essentially improve the temperature function. The average temperature is reproduced well and the mean scatter in particular cells is less than 10%. A similar analysis made for K confirms that K greater than 3 does not improve significantly the model function. For all further investigations we use the temperature function T with $N=6$ and $K=3$. However, Fig. 1 suggests that a second order approximation in N gives already an approximation with 15%.

Temperature Distribution

The model function $T(\theta, \phi)$ is presented in Figs. 2 and 3 at two fixed heights at 1500 LT and 0300 LT, respectively. The latitudinal distribution derived earlier by several authors (Brace, 1970; Spenner and Dumbs, 1974; Dorling and Raitt, 1976) is reproduced in the global distribution derived in this study. In addition a longitudinal distribution occurs. One may argue that a longitudinal distribution is only the result of temporal variations. Figures 2 and 3, however, demonstrate clearly that the general longitudinal pattern is quite similar at different heights and during day and nighttime. Ten thousand independent measurements cannot produce such a consistent picture without a geophysical source.

The longitudinal distribution of the model function is shown in more detail (at 500 km altitude) in Figs. 4 and 5. The highest longitudinal temperature variation is approximately 400 K along a fixed magnetic latitude in the southern hemisphere at 1500 LT. The variations at other latitudes are usually between 100 and 300 K. Low temperatures are obtained between 60° and 140° geomagnetic longitude in the southern hemisphere and between 260° and 360° in the northern hemisphere. At 0300 LT the longitudinal variation along a fixed
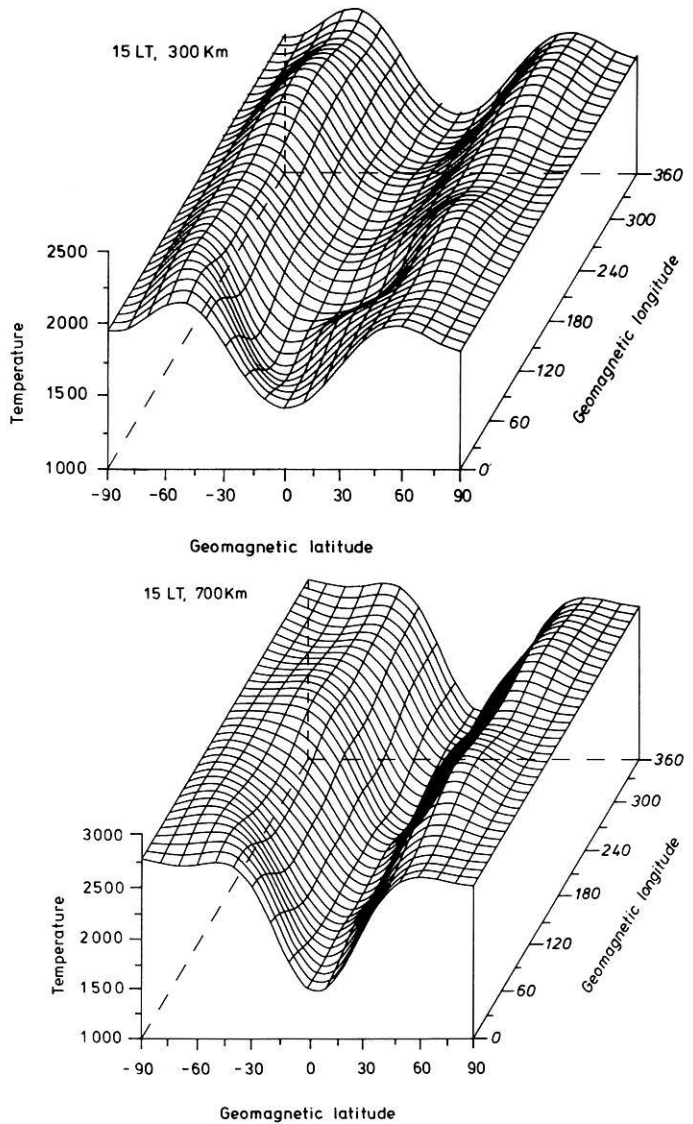
15 LT, 300 Km

15 LT, 700Km

Fig. 2. Model distribution at 1500 LT for 700 and 300 km

magnetic latitude is also well pronounced. The locations of high and low temperature are close to that observed 1500 LT. A longitudinal variation of the neutral gas density was recently reported by von Zahn and Fricke (1978). Comparing the electron temperature variation with the neutral Argon density variation along a fixed latitude range we find that a high electron temperature occurs on locations with a low Argon density.

At 1500 LT the latitudinal temperature distribution shows a deep minimum close to the equator (Fig. 4) at 500 km. In contrast to the daytime distribution there are two small minima on both sides of the equator (Fig. 5) at 0300 LT.
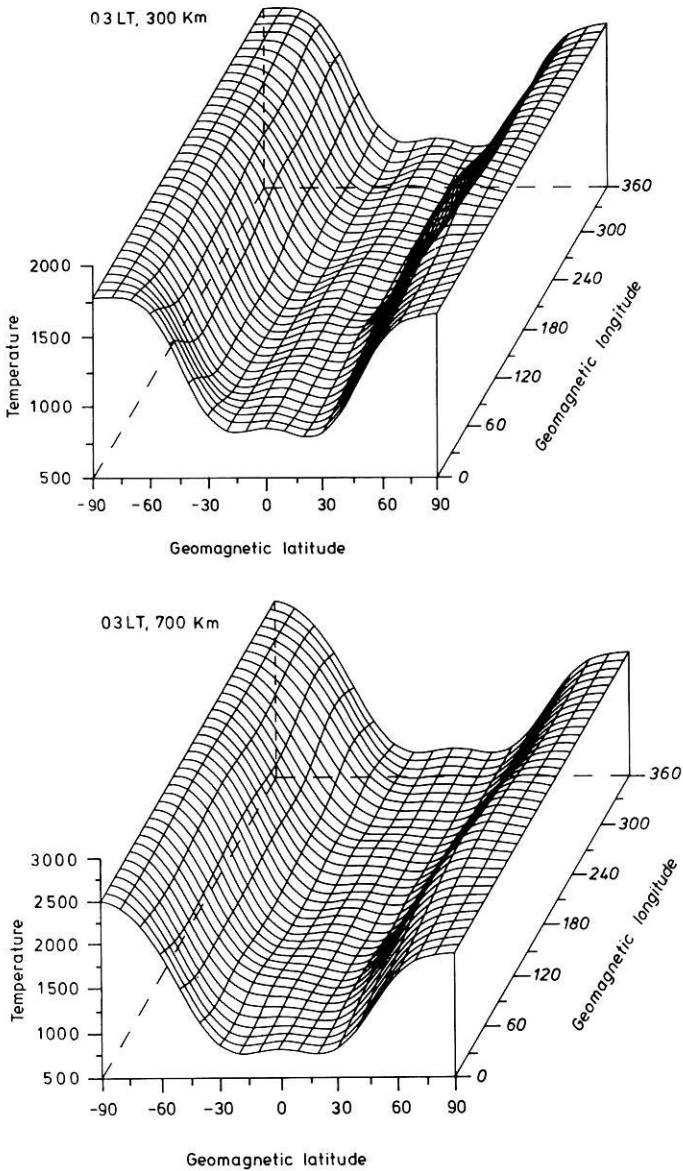
Fig. 3. Model distribution at 0300 LT for 700 and 300 km

The latitudinal and height variation of the temperature is given in Figs. 6 and 7 at 0° geomagnetic longitude. The isotherms at 1500 LT indicate a temperature minimum at approximately 400 km altitude at low latitudes. Little variation with altitudes may be in small error because the data required to derive a height variation were obtained over a relatively long time period under different geophysical conditions. The isotherms represent the averaged distribution in a three months period but they may possibly not reproduce well details in a height profile.
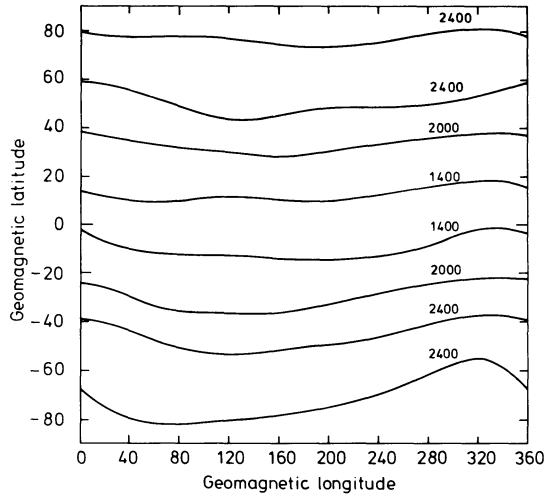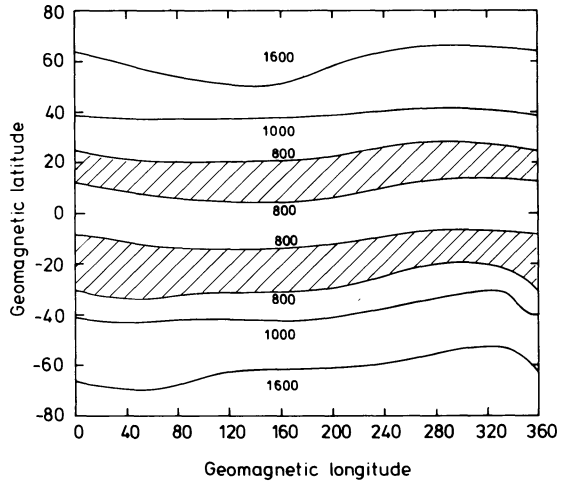
Fig. 4. Isotherms at 500 km altitude and 1500 LT

Fig. 5. Isotherms at 500 km altitude and 0300 LT

Intercomparison Between Model and Measurements

We calculated the model temperatures for all individual measurements and compared them with each other. To evaluate how well the model represents the data we have calculated the model temperature for each data point and compared it to the measurement. To demonstrate that the model represents the latitudinal variation adequately, we have determined the mean deviation of the measured values from the model values at different latitudes for both 1500 LT and 0300 LT. The calculated mean difference $\overline{\Delta T}$ between all AEROS measurements and the model was less then 30 K. This confirms that the computed parameters a_{knm} are satisfactory, and that the model function represents the
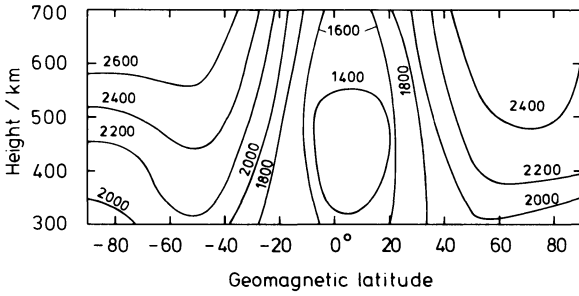
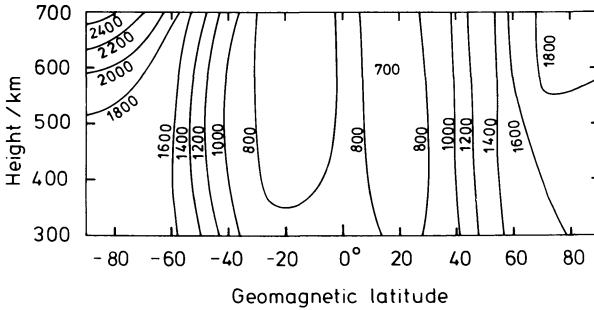**Fig. 6.** Isotherms at 0° geomagnetic longitude and 1500 LT

Fig. 7. Isotherms at 0° geomagnetic longitude and 0300 LT

global mean value of the measurements. A more detailed analysis has to demonstrate whether the model describes the mean value of selected data at different latitudes well enough and to determine how large the scatter in the measurements is. For this purpose we determined the mean deviation d_D according to Eq. (3) for different latitudes. δ in Eq. (3) is the difference between the measured temperature and the model function at the same location divided by the model-temperature. The d_D-value gives a relative mean scatter of 7% integrated over all longitudes for the first 100 days in 1973.

Figures 8 and 9 show the boundaries of the determined mean deviations for different latitudes. It is evident that the data spread is increased at higher latitudes. These relative variations during night (Fig. 9) are much higher than during day (Fig. 8) with the exception of the equatorial area. The daytime model is a few percent too high at low latitudes and too low at midlatitudes. Areas with strong temperature gradients are smoothed a little. These small deviations of the average values are not of great importance since the temporal variations given by the scatter are much larger. The uncertainty in predicting temperatures is mainly given by the scatter of particular measurements. The calculated d_D value varies only slightly during the AEROS-A mission period of eight months and does not change the general behavior.

The model function represents an average temperature during the time period considered. Differences ΔT between particular data and the model may reflect geophysical events during a few day period or seasonal and annual effects for a longer time period. We tried to find possible relations between the temperature differences $\overline{\Delta T}$ and geophysical indices. To this end we correlated
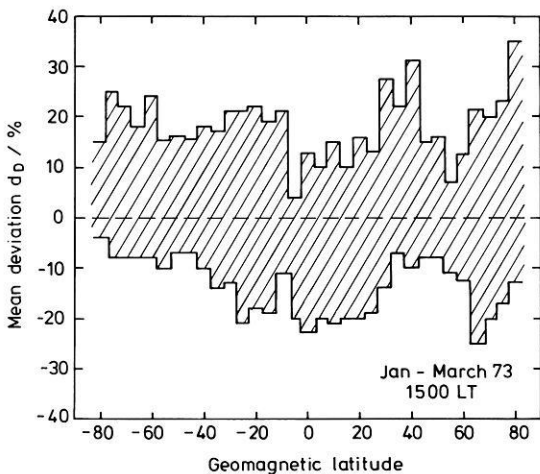
Fig. 8. Mean deviation between model and measured data points at 1500 LT
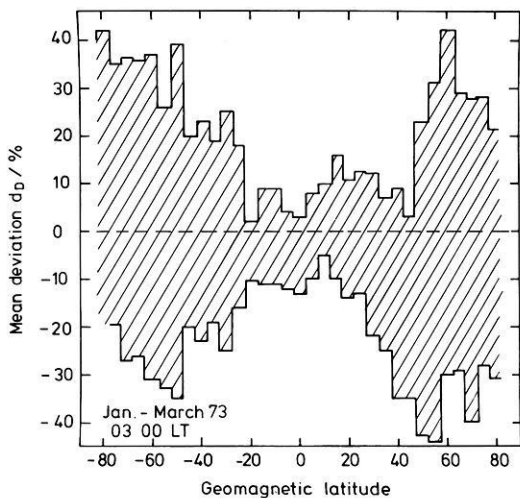
Fig. 9. Mean deviation between model and measured data points at 0300 LT

$\overline{\Delta T}$ with the K_p-value, the A_p-value and with the sunspot number during the eight months period. The analysis was done for different geomagnetic latitude ranges. The result did not show any correlation between these indices. This indicates clearly that the temperatures do not follow the indices in a simultaneous and clear relation. It confirms an earlier investigation (Spenner, 1975), which did not show a significant relation between K_p and electron temperature.

Monthly mean temperature differences $\overline{\Delta T}$ were used to search for a seasonal or annual variation. To obtain data for a period of one year for a Fourier analysis, the measurements of one hemisphere were used again six months later at the other hemisphere mirrored at the geographic equator. This procedure can only provide a rough indication of the annual variation when no complete period of measurement is available. The calculated Fourier coefficients

Fig. 10. Relative frequency of measurements observed outside the σ_M boundary

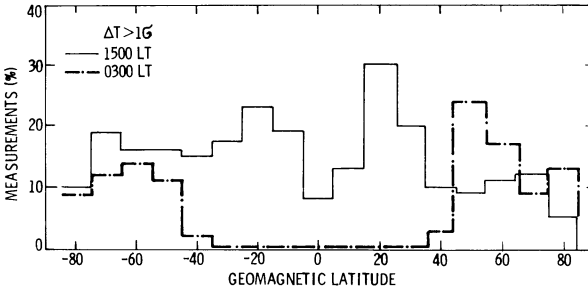did not show a significant annual or seasonal period either at low, middle or high latitudes. This means that the model function determined for January to March, 1973, must be valid for the second part of the AEROS-A mission from April to August, 1973. Indeed the calculated mean deviation d_D for the period was not considerably different from the values shown already in Figs. 8 and 9. Seasonal and annual effects must be smaller than short time or local changes. As a consequence we argue that these effects do not exceed 15 % during low solar activity.

Individual data points are sometimes far away from the mean temperature value. A few such values considerably increase the mean deviation $(\overline{\Delta T})$ $= 1/n \Sigma |\Delta T|$ and the standard deviation σ between model and measurements. The determined σ_M value between particle measurements and the mean temperature was 440 K and 490 K for day and nighttime, respectively, where

$$\sigma_M^2 = \frac{\Sigma (T - \overline{\Delta T})^2}{n_R} \tag{4}$$

n_R = number of measurements in a particular cell range. The spread in ΔT does not follow a statistical error distribution. At 1500 LT more than 80 % and at 0300 LT more than 90 % of all measurements are within the 1 σ range (where as for a Gaussian distribution one expects only 60 %). Most of the runaways are probably caused by extreme geophysical conditions and restricted to a particular area. Temperatures which differ more than 1 σ from the model are considered to be outside of quiet or usual conditions.

The temperatures outside the σ_M boundary are used to look for areas, where data spread may occur. To this end, we determined the percentage of spread values relative to all measurements as a function on geomagnetic latitude and longitude. Figure 10 shows small peaks with more than 20 % of spread data at about 20° latitude of both sides of the equator at 1500 LT. At 0300 LT all the spread temperatures occur in an area around 60° latitude.

A corresponding analysis of the spread data for different geomagnetic longitudes indicate peaks at 60° and 170° longitude during daytime. The peaks seem to be higher than the expected random noise at 1500 LT.

Summary and Conclusions

The empirical model based on the AEROS-A data predicts electron temperatures for 0300 LT and 1500 LT. Temperatures can be calculated worldwide either with geographic or geomagnetic coordinates between 300 and 700 km altitude. The model temperature is in quite good agreement with ground observations done by incoherent radar scatter technique. This is demonstrated in a second paper (Spenner et al., 1979). The model temperatures are considerably lower than the values predicted by the ESRO 4 model (Dorling and Raitt, 1976), though both measurements were taken at the approximately same time period. The observed longitudinal variations show maxima of the electron temperature in areas where the density of neutral Argon observed by the ESRO 4 gas analyzer (von Zahn and Fricke, 1978) exhibits a minimum in the northern hemisphere ($\approx 120°$, geomag. long.) and southern hemisphere ($\approx 320°$ geomag. long.). The temperature minima are located as well where the neutral density maximum of Argon occurs with the exception of the South Atlantic anomaly region.

Appendix

1. Spherical Harmonics

The oscillation of a sphere can be described by the differential equation

$$\Delta U = \frac{1}{c^2} \frac{\partial^2 U}{\partial t^2} \tag{I}$$

where U is the wave function, c is the wave velocity, and t the time. U may be written in the form

$$U = F(r, \theta, \phi) \cdot T(t)$$

where r is the radius of the sphere, θ the latitude and ϕ the longitude. We are interested only in the part of a solution of Eq. (I) depending on θ and ϕ. It can be shown that this part follows the differential equation.

$$\frac{1}{\cos \theta} \frac{\partial}{\partial \theta} \left(\cos \theta \frac{\partial Y}{\partial \theta} \right) + \frac{1}{\cos^2 \theta} \frac{\partial^2 Y}{\partial \phi^2} + \alpha Y = 0 \tag{II}$$

where Y depends only on θ and ϕ, α is constant in θ, ϕ.

All the algebraic (in $\cos \theta$, $\cos \phi$) solutions of Eq. (II) are given by the spherical harmonics Y_{nm} of the form

$$Y_{n,m}(\theta, \phi) = \sin^{|m|} \theta \, \frac{d^{|m|} P_n(\cos \theta)}{(d \cos \theta)^{|m|}} \cdot e^{\pm im\phi} \cdot C_{nm} \tag{III}$$

where P_n is the Legendre polynomial of order n and C_{nm} is a normalizing factor. Replacing the exponential term by sin and cos functions in (III) and normalizing the spherical harmonics so that they are 1 at the north pole (Bronstein-Semendjajew, 1956) we get

$$Y_{nm}(\theta, \phi) = C_{nm} \sin^{|m|} \phi \cdot \frac{d^{|m|}}{d(\cos \theta)^{|m|}} P_n(\cos \theta) \cdot R_m(\phi)$$

where

$$R_m(\phi) = (-1)^m \cdot \begin{array}{ll} \sin m\phi & \text{for } m < 0 \\ \cos m\phi & \text{for } m \geq 0, \end{array}$$

$$C_{nm}^2 = \frac{(n-|m|)!}{(n+|m|)!} \cdot \frac{1}{4\pi} \tag{IV}$$

The integral over the volume Ω becomes

$$\oint Y_{nm} \cdot Y_{n'm'} \, d\Omega = \delta_{nn'} \cdot \delta_{mm'} \tag{V}$$

because the Eigensolutions of differential equations are orthogonal.

2. Functions in Height

The temperature can be described as

$$T(h, \theta, \phi) = \sum_{k=0}^{K} \sum_{n=0}^{N} \sum_{m=-n}^{n} a_{knm} Y_{nm}(\theta, \phi) \cdot F_k(h) \tag{VI}$$

where Y_{nm} are the spherical harmonics as defined by Eq. (IV) and F_k are polynomials in h of degree k. Any function T can be expressed in such a series expansion.

For easy computation of the a_{knm} we desire that (see later, computation of the a_{knm})

$$I = \int Y_{nm} F_k \cdot Y_{n'm'} F_{k'} \, d\tau = \delta_{mm'} \delta_{nn'} \delta_{kk'}. \tag{VII}$$

The integral becomes with Eq. (V)

$$I = \oint_{\Omega, h} Y_{nm} Y_{n'm'} \cdot F_k \cdot F_{k'} h^2 \, dh \, d\Omega$$

$$= \delta_{nn'} \delta_{mm'} \int_{h_1}^{h_2} h^2 F_k F_{k'} \, dh$$

and with (VII) we get

$$\int_{h_1}^{h_2} h^2 F_k F_{k'} \, dh = \delta_{kk'} \tag{VIII}$$

where h_2 and h_1 are the boundaries of the considered height interval.

The expansion of the F_k is

$$F_0 = a_{00}$$

$$F_1 = a_{10} + a_{11} h.$$

$$\ldots$$

$$F_n = a_{n0} + a_{n1} h + \ldots a_{nn} h^n.$$

Eq. (VII) yields for $k = k' = 0$

$$a_{00} = \frac{1}{\sqrt{\int_{h_1}^{h_2} h^2 \, dh}}$$

and

$$a_{00} \cdot \int_{h_1}^{h_2} (a_{10} + a_{11} h) h^2 \, dh = 0 \quad \text{for } k' = 0, \ k = 1$$

$$\int_{h_1}^{h_2} (a_{10} + a_{11} h)^2 h^2 \, dh = 1 \quad \text{for } k = k' = 1$$

Table 1

h	n	m	a_{knm} (1500 LT)	a_{knm} (0300 LT)
0	0	0	$9290\,E+1$	$4976\,E+1$
1	0	0	$6506\,E+0$	$1651\,E+0$
2	0	0	$2826\,E-1$	$6561\,E-1$
3	0	0	$-1044\,E+0$	$-2054\,E-1$
0	1	-1	$5462\,E-1$	$-3974\,E-1$
1	1	-1	$-2884\,E-1$	$-2404\,E-1$
2	1	-1	$8509\,E-2$	$-6016\,E-2$
3	1	-1	$-8540\,E-2$	$-4226\,E-2$
0	1	0	$-1087\,E+0$	$-8254\,E-2$
1	1	0	$-1080\,E-1$	$-6363\,E-1$
2	1	0	$-1542\,E-1$	$-6671\,E-1$
3	1	0	$3420\,E-1$	$-2064\,E-1$
0	1	1	$-3246\,E-1$	$3363\,E-1$
1	1	1	$1006\,E-1$	$-6907\,E-2$
2	1	1	$3788\,E-1$	$-1126\,E-1$
3	1	1	$-8795\,E-2$	$3128\,E-2$
0	2	-2	$-4113\,E-1$	$-4121\,E-1$
1	2	-2	$-5864\,E-2$	$5811\,E-2$
2	2	-2	$1255\,E-1$	$1958\,E-1$
3	2	-2	$-5917\,E-2$	$1178\,E-1$
0	2	-1	$-2183\,E+0$	$-2973\,E+0$
1	2	-1	$-5367\,E-2$	$6294\,E-2$
2	2	-1	$2327\,E-1$	$3924\,E-1$
3	2	-1	$8651\,E-2$	$-4952\,E-2$
0	2	0	$1735\,E+1$	$1684\,E+1$
1	2	0	$1680\,E+0$	$2337\,E+0$
2	2	0	$-1453\,E+0$	$6999\,E-1$
3	2	0	$6019\,E-1$	$-2839\,E-3$
0	2	1	$3356\,E+0$	$1802\,E+0$
1	2	1	$5824\,E-1$	$9037\,E-2$
2	2	1	$-6681\,E-1$	$2208\,E-1$
3	2	1	$4200\,E-2$	$-4697\,E-2$
0	2	2	$5769\,E-1$	$-2481\,E-1$
1	2	2	$1343\,E-1$	$-1254\,E-1$
2	2	2	$-1604\,E-1$	$6481\,E-2$
3	2	2	$-1403\,E-1$	$-2056\,E-2$

This is a linear homogeneous equation which yields a linear relation between a_{10} and a_{11}, and a quadratic equation for a_{10}. In analogous manner one can successively compute the coefficients a_k for higher degrees.

In the case of $h_1=3$ and $h_2=7$ (normalized to 100 km) it becomes

$$F_0 = 0.86066 \cdot 10^{-1}$$
$$F_1 = -0.3965 + 0.6910 \cdot 10^{-1} h$$
$$F_2 = 1.5203 - 0.6105 h + 0.575 \cdot 10^{-1} h^2$$
$$F_3 = -6.6602 + 4.254 h - 0.8616 h^2 + 0.55783 \cdot 10^{-1} h^3 \tag{IX}$$

3. Computation of a_{knm}

The derived orthogonal function Y_{nm} and F_k allows us to derive easily the series expansion parameters a_{knm}.

Equation (VI) multiplied by $Y_{n'm'}F_{k'}$ becomes

$$T Y_{n'm'}F_{k'} = Y_{n'm'}F_{k'} \sum_{k,n,m} a_{knm} \cdot F_k.$$

Integration over $d\tau$ yields

$$\int T Y_{n'm'}F_{k'}\, d\tau = \int \sum_{k,n,m} a_{knm} Y_{nm} Y_{n'm'} F_k F_{k'}\, d\tau$$

$$= \sum_{k,n,m} a_{knm} \int Y_{nm} \cdot Y_{n'm'}\, d\Omega \int h^2 F_k \cdot F_{k'}\, dh$$

It becomes with use of Eqs. (V) and (VIII)

$$\int T Y_{n'm'}F_{k'}\, d\tau = a_{k'n'm'} \tag{X}$$

The a_{knm} values from the AEROS-A measurements determined by Eq. (X) and using the mean temperature data as described earlier are listed in Table 1. The table presents the a_{knm} coefficients up to the second order in N, M and the third order in K. A better approximation can be achieved by higher order in N, M as demonstrated in Fig. 1.

References

Brace, L.H.: The global structure of ionosphere temperature. Space Res. **10**, 633–651, 1970

Bronstein-Semendjajew: Taschenbuch der Mathematik, S. 401. Moskau: Staatlicher Verlag für technisch-theoretische Literatur 1956

Dorling, E.B., Raitt, W.J.: Electron temperature models of the thermosphere to 1,100 km based on ESRO-4 measurements. Planet. Space Sci. **24**, 739–747 (1976)

Hedin, A.E., Mayr, H.G., Reber, C.A., Spencer, N.W., Carignan, G.R.: Empirical model of global thermospheric temperature and composition based on data from the Ogo 6 quadrupole mass spectrometer. J. Geophys. Res. **79**, 215–225 (1974)

Schunk, R.W., Nagy, A.F.: Electron temperatures in the *F*-region of the ionosphere: Theory and observations. Rev. Geophys. Space Phys. **16**, 355–399 (1978)

Spenner, K.: Quiet and disturbed electron temperature and density at different latitudes during daytime. Space Res. **15**, 363–368 (1975)

Spenner, K., Bilitza, D., Plugge, R.: Intercomparison between AEROS electron temperature model and mean temperature profiles of different incoherent scatter radar stations. J. Geophys. **46**, 57–61 (1979)

Spenner, K., Dumbs, A.: The retarding potential analyzer on AEROS-B. J. Geophys. **40**, 585–592 (1974)

Spenner, K., Dumbs, A., Lotze, W., Wolf, H.: Correlation between daytime electron temperature and density variations at low latitudes. Space Res. **14**, 259–263 (1974)

Spenner, K., Plugg, R.: Electron temperature model derived from AEROS-A. Space Res. **18**, 241–244 (1978)

Zahn, U. von, Fricke, K.H.: Empirical models of global thermospheric composition and temperature during geomagnetically quiet times compared with ESRO 4 gas analyzer data. Rev. Geophys. Space Phys. **16**, 169–175 (1978)